Two-folds in nonsmooth dynamical systems

Mike R Jeffrey [*]

[*] *Dept. of Engineering Mathematics, University of Bristol, Queen's Building, Bristol BS8 1TR, UK. email: mike.jeffrey@bristol.ac.uk*

Abstract: In a three dimensional dynamical system with a discontinuity along a codimension one switching manifold, orbits of the system may be tangent to both sides of the switching manifold generically at isolated points. It is perhaps surprising, then, that examples of such 'two-fold' singularities are difficult to find amongst physical models. They occur where the relative curvature between the flow field and the switching manifold is nonsymmetric about the discontinuity. Here we motivate their study with a local form model of nonlinear control that exhibits the two-fold singularity, where the flow is constant either side of a curved switching manifold. We describe the local dynamics around general two-fold singularities, then consider their effect on global dynamics via one parameter bifurcations of limit cycles.

1. INTRODUCTION

Piecewise-smooth vector fields model switching and non-linearity everywhere from relay and control systems to economics and neurophysiology. Recent studies of their dynamics has shown *grazing singularities* that form organising centers of stability, such as limit cycle bifurcations described by di Bernardo et al. (2008) and routes to chaos described by Galvanetto (1997); di Bernardo et al. (1998); Zhusubalyev and Mosekilde (2003).

The novelty of piecewise-smooth systems is the dynamics made possible by the presence of a *switching manifold*, which separates regions of smooth dynamics. Of chief interest are sliding modes – where the system slides along the switching manifold – and the boundaries of sliding modes. These boundaries are where orbits *graze* the surface, poised on the boundary between smooth and nonsmooth dynamics. In the singularity literature *grazing points* are referred to as "*folds*".

In three dimensions, grazing occurs either side of the switching manifold along curves. It is common in control to design these curves as parallel straight lines, with a strip of sliding motion in between. But nonlinearities, such as in a general Lur'e system (Lur'e and Postnikov (1944)), or arising through noise or imprecision in design, may cause deviations. It is then sensible to ask whether a system is robust to such small deviations from the ideal model.

It is easy to see that if the two grazing (or fold) lines are perturbed, even a small amount, then they may bend and even intersect. This may arise from perturbations of the vector fields, or curvature of the switching manifold. Indeed, such an intersection is generic in systems of at least three dimensions, as proven by Teixeira (1990). With very little analysis the striking implications of such "two-fold" points is unveiled, and we describe this briefly here.

A two-fold is a codimension two set where orbits graze both sides of a smooth switching manifold. Here all of the key features of a piecewise-smooth system are present:

orbits that cross the manifold, orbits that slide along it according to Filippov's rule, and orbits in unstable sliding.

A body of work for piecewise-smooth systems now exists regarding their global dynamics, see for example Kunze (2000); Leine and Nijmeijer (2004); Kowalczyk and di Bernardo (2005); di Bernardo et al. (2008). The same is true of their singularities, described predominantly by Teixeira (1993). But so far little systematic attempt has been made to bring the two ingredients together and understand the dynamics caused by the singularities. We address this here for the generic two-fold singularity. The class of two-folds includes the Teixeira singularity described first by Teixeira (1990). This theoretically irksome case is obtained by relaxing certain symmetry constraints common in relay systems, that otherwise constrain two-fold grazing to occur along a single degenerate curve.

We motivate this paper with a model from nonlinear control, a class of functions

$$\dot{\mathbf{x}} = \dot{\mathbf{x}}^i = \mathbf{a}^i + \mathbf{g}^i(\mathbf{x}), \qquad \mathbf{x} \in \mathbb{R}^3 \qquad (1)$$

where $i = \mathsf{R}$ labels the 'right' region $h(\mathbf{x}) > 0$ and $i = \mathsf{L}$ the 'left' region $h(\mathbf{x}) < 0$, for a monotonic scalar function h, vector constants $\mathbf{a}^i$ and smooth polynomials $\mathbf{g}^i$ that satisfy $\mathbf{g}^i(\mathbf{0}) = \mathbf{0}$. At a two-fold point we have $\dot{h} = 0$ for the Lie derivatives $\dot{h} = \dot{\mathbf{x}}^\mathsf{R} \cdot \nabla h$ and $\dot{h} = \dot{\mathbf{x}}^\mathsf{L} \cdot \nabla h$ evaluated along both the L and R flows. This implies that

$$\mathbf{a}^R \cdot \nabla h = \mathbf{a}^L \cdot \nabla h = 0. \qquad (2)$$

We can neglect the polynomial term $\mathbf{g}$ if we allow a quadratic switching manifold, for instance $h = \xi + c_1\eta^2 + c_2\zeta^2 + c_3 yz = 0$ in coordinates $\mathbf{x} = (\xi, \eta, \zeta)$. Up to arbitrary scaling the c_i coefficients can be reduced to two parameters α, β, and we have the (Morse) switching surface:

$$h(\xi, \eta, \zeta) = \xi + \tfrac{1}{2}\alpha\eta^2 + \tfrac{1}{2}\beta\zeta^2 + yz \qquad (3)$$

Figure 1 illustrates such a switching manifold, and the vector fields either side of it.

In section 2 we show that this is equivalent to the normal form for a two-fold, and derive the sliding vector field on
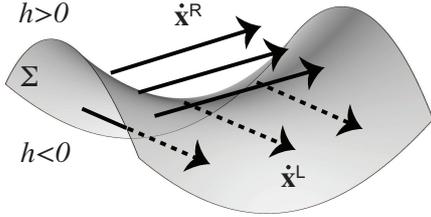
Fig. 1. Switching at a saddle surface: a piecewise-constant dynamical system that jumps at $h = 0$. Here h has the form $h \sim x + y^2 - z^2$.

the switching manifold. In sections 4-6 we describe the sliding dynamics, and infer from it four qualitatively different classes of one-parameter bifurcations that catastrophically destroy limit cycles. These mechanisms, which we refer to here as *catastrophic sliding bifurcations*, can occur in any Filippov system when a limit cycle intersects the boundary of an unstable sliding region.

2. THE TWO-FOLD PROBLEM

Let us consider a piecewise-smooth vector field of the form
$$\dot{\mathbf{x}} = \left\{ \begin{array}{ll} \dot{\mathbf{x}}^R(\mathbf{x}), & h(\mathbf{x}) > 0 \\ \dot{\mathbf{x}}^L(\mathbf{x}), & h(\mathbf{x}) < 0 \end{array} \right\}. \quad (4)$$
The switching manifold Σ is typically expressed as the zero-contour of the scalar function h,
$$\Sigma = \left\{ \mathbf{x} \in \mathbb{R}^3 : h(\mathbf{x}) = 0 \right\}. \quad (5)$$
In $\mathbb{R}^3$ there generically exists an isolated point $p \in \Sigma$ at which $\dot{\mathbf{x}}$ is tangent to both sides of Σ. That is, letting $\dot{h}^i$ denote the Lie derivative $\dot{\mathbf{x}}^i \cdot \nabla h(\mathbf{x})$,
$$\dot{h}^R = \dot{h}^L = 0 \quad \text{at} \quad \mathbf{x} = \mathbf{x}_p. \quad (6)$$
The nondegeneracy conditions $\dot{h}^i \neq 0$ must be satisfied at p, guaranteeing that the tangency is of quadratic order. This is the two-fold singularity described by Teixeira (1990) and Jeffrey and Colombo (2009). The tangency sets
$$\begin{array}{l} S^R = \left\{ \mathbf{x} \in \Sigma : \dot{h}^R = 0 \right\} \\ S^L = \left\{ \mathbf{x} \in \Sigma : \dot{h}^L = 0 \right\} \end{array} \quad (7)$$
must intersect tranversally. Using (3) we have $\dot{h} = \dot{\xi} + (\alpha\eta + \zeta)\dot{\eta} + (\eta + \beta\zeta)\dot{\zeta}$. From (2) we have $\dot{\xi} = \dot{\mathbf{x}} \cdot \nabla h \approx 0$. Without loss of generality, choose the local coordinates so that at $\mathbf{x}_p$ we have $(\dot{\eta}, \dot{\zeta}) = (0, -\lambda, 0)$ for R and $(\dot{\eta}, \dot{\zeta}) = (0, 0, \mu)$ for L. Finally define new coordinates
$$\begin{pmatrix} x \\ y \\ z \end{pmatrix} = \begin{pmatrix} h \\ \alpha\eta + \zeta \\ \eta + \beta\zeta \end{pmatrix}, \quad (8)$$
with the result that $(\dot{x}, \dot{y}, \dot{z}) = (-y, \alpha, 1)$ for $x > 0$ and $(\dot{x}, \dot{y}, \dot{z}) = (z, 1, \beta)$ for $x < 0$. It is more convenient to define $w = 1/\alpha$ and $v = 1/\beta$, then make an arbitrary rescaling to obtain
$$\begin{pmatrix} \dot{x} \\ \dot{y} \\ \dot{z} \end{pmatrix} = \left\{ \begin{pmatrix} -y \\ \lambda \\ \lambda v \end{pmatrix} \text{ for } x > 0, \begin{pmatrix} z \\ \mu w \\ \mu \end{pmatrix} \text{ for } x < 0 \right\}. \quad (9)$$
Our geometric construction must be relaxed to allow different arrows of time, given by a free choice of signs $\lambda, \mu = \pm 1$. This leads to three distinct cases, $\lambda = \mu = -1$, $\lambda = -\mu = +1$, $\lambda = \mu = 1$ (the two cases where $\lambda = -\mu = \pm 1$ are equivalent), and in sections 4-6 we consider the dynamics in each case.

The system (9) is equivalent to the two-fold normal forms defined by Teixeira (1993) with a flat switching manifold.

Finally, we say the tangency/grazing of the vector field/flow, to Σ, is

- visible if $\ddot{h}^R > 0$ or $\ddot{h}^L < 0$, and
- invisible if $\ddot{h}^R < 0$ or $\ddot{h}^L > 0$.

This local approximation captures the leading order behaviour of the two-fold system, drawing together the results of Teixeira (1990, 1993) with Jeffrey and Colombo (2009), and implying mechanisms for limit cycle destruction inherent in the local geometry that extends the global analysis of Kowalczyk and di Bernardo (2005).

3. SLIDING DYNAMICS

In the piecewise-smooth system (9), the *tangency sets* $S^{R,L}$ partition our planar switching manifold Σ into four quadrants:
$$\begin{array}{l} \Sigma^{sl} = \left\{ \mathbf{x} \in \Sigma : y, z \geq 0 \right\} \\ \Sigma^{esc} = \left\{ \mathbf{x} \in \Sigma : y, z \leq 0 \right\} \\ \Sigma^{cr} = \left\{ \mathbf{x} \in \Sigma : yz < 0 \right\}. \end{array} \quad (10)$$
In the two crossing regions Σ^{cr} orbits cross the switching manifold continuously but nondifferentiably, from $h > 0$ to $h < 0$ in $\{\Sigma^{cr} : z < 0 < y\}$, from $h < 0$ to $h > 0$ in $\{\Sigma^{cr} : y < 0 < z\}$. In the sliding region Σ^{sl} both vector fields $\mathbf{x}^{R,L}$ point towards Σ, in the escaping region Σ^{esc} both vector fields $\mathbf{x}^{R,L}$ point away from Σ, then in either case according to the Filippov convention (Filippov (1988)) the dynamics is given by the convex combination

$$\dot{\mathbf{x}} = \frac{(\nabla h \cdot \dot{\mathbf{x}}^L) \dot{\mathbf{x}}^R - (\nabla h \cdot \dot{\mathbf{x}}^R) \dot{\mathbf{x}}^L}{\nabla h \cdot (\dot{\mathbf{x}}^L - \dot{\mathbf{x}}^R)}, \quad \mathbf{x} \in \Sigma^{sl,esc}. \quad (11)$$

This vector field is confined to the $h = 0$ plane, so we write it as $\dot{\mathbf{x}} = \mathbf{F}$ and ignore the vanishing h (or x) component, leaving

$$\mathbf{F} = \frac{1}{z+y} \begin{pmatrix} \mu w & \lambda \\ \mu & \lambda v \end{pmatrix} \begin{pmatrix} y \\ z \end{pmatrix}. \quad (12)$$

The 2×2 matrix in (12) has determinant
$$\Delta = \mu\lambda(vw - 1), \quad (13)$$
and eigenvectors $\mathbf{d}_\pm$ and eigenvalues $\delta_\pm$ given by

$$\mathbf{d}_\pm = \begin{pmatrix} \lambda \\ \delta_\pm - \mu w \end{pmatrix} = \begin{pmatrix} \delta_\pm - \lambda v \\ \mu \end{pmatrix} \quad (14)$$

$$\delta_\pm = \frac{1}{2} \left(\lambda v + \mu w \pm \sqrt{(\lambda v - \mu w)^2 + 4\lambda\mu} \right). \quad (15)$$

The quantities $\Delta, \mathbf{d}_\pm, \delta_\pm$, describe the Jacobian of the 'normalised' sliding vector field
$$\hat{\mathbf{F}} = (y + z) \mathbf{F} \quad (16)$$
which has a fixed point at the origin that is hyperbolic provided that $vw \neq 1$. The Filippov field $\mathbf{F}$ has the same phase portrait (same orbits) as this normalised field $\hat{\mathbf{F}}$ except that: the regions Σ^{cr} are excluded, the two-fold point is reached in finite time, and the time direction in Σ^{esc} is reversed. If the normalised vector field has a saddlepoint or node at the origin, we say the Filippov field is "saddle-like" or "node-like". We will now discuss the different cases arising from $\lambda, \mu = \pm 1$.

4. THE VISIBLE TWO-FOLD
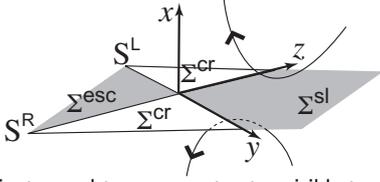
Fig. 2. Coordinates and tangency sets at a visible two-fold.

A vector field with transverse visible tangency sets (figure 2) has the local form

$$\begin{pmatrix} \dot{x} \\ \dot{y} \\ \dot{z} \end{pmatrix} = \left\{ \begin{pmatrix} -y \\ -1 \\ -v \end{pmatrix} \text{for } x > 0, \begin{pmatrix} z \\ -w \\ -1 \end{pmatrix} \text{for } x < 0 \right\} \quad (17)$$

which is the system in section 1 with $\lambda = \mu = -1$. The sliding vector field quantities (13-15) become:

$$\begin{aligned} \Delta &= wv - 1 \\ \mathbf{d}_\pm &= \begin{pmatrix} -1 \\ \delta_\pm + w \end{pmatrix} = \begin{pmatrix} \delta_\pm + v \\ -1 \end{pmatrix} \\ \delta_\pm &= \tfrac{1}{2}\left(-v - w \pm \sqrt{(v-w)^2 + 4} \right). \end{aligned} \quad (18)$$

The eigenvalues $\delta_\pm$ are both real and satisfy $\delta_+ > -w$, $\delta_- > -v$. By comparing this with the two (equivalent) expressions given here for $\mathbf{d}_\pm$, we infer that the $\mathbf{d}_+$ direction lies in the crossing regions Σ^{cr}, while the $\mathbf{d}_-$ direction lies in the sliding/escaping regions Σ^{sl} or Σ^{esc}.

Figure then 3(i) shows dynamics on Σ for the saddle-like case $vw < 1$, for which $\mathbf{d}_-$ is the attractive eigendirection. There are two node-like cases $vw > 1$: figure 3(ii), if $\delta_\pm < 0$ the origin is an attractive node-like singularity with $|\delta_-| > |\delta_+|$; figure 3(iii), if $\delta_\pm < 0$ the origin is a repelling node-like singularity with $|\delta_-| < |\delta_+|$.
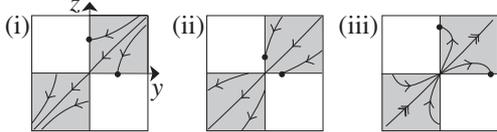
Fig. 3. The sliding vector field near a visible two-fold, implied by (18). Dots indicate ejection points, double arrows indicate the weak eigendirection. The cases are: (i) the saddle-like case $vw < 1$, (ii) the node-like case with $vw > 1$ and $v, w > 0$, (iii) the node-like case with $vw > 1$ and $v, w < 0$.

Consider now the system (17) to be the local approximation of a global system where a limit cycle grazes Σ near a two-fold singularity. Let us assume the limit cycle resides entirely within $x \geq 0$, with a single point of contact that must lie along the line S^R. Note that S^R borders both Σ^{sl} and Σ^{esc}. The global system is not generic: under perturbation the limit cycle will no longer graze, it may either lose contact with Σ or impact Σ transversally. Grazing therefore constitutes the degenerate point of a bifurcation, which we can unfold with a single global parameter.

Consider first a limit cycle that grazes on the half-line $\{\mathsf{S}^\mathsf{R} : z > 0\}$, where the conditions $\dot{h}^\mathsf{R} = 0$, $\ddot{h}^\mathsf{R} > 0$, $\dot{h}^\mathsf{L} > 0$ are satisfied. This means that a limit cycle grazing along S^R where it borders Σ^{sl} undergoes the grazing-sliding bifurcation described by Kowalczyk and di Bernardo (2005): on one side of the bifurcation a smooth orbit resides in $x > 0$, on the other side it takes on a sliding

segment in Σ^{sl} and is ejected back into $x > 0$ along S^R. Due to the attractivity of the sliding region it is known that limit cycles persist under such sliding bifurcations.
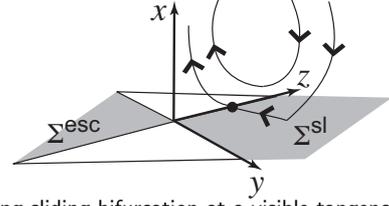
Fig. 4. Grazing-sliding bifurcation at a visible tangency.

If the limit cycle grazes instead along $\{\mathsf{S}^\mathsf{R} : z < 0\}$ on the border of Σ^{esc}, we have the conditions

$$\dot{h}^\mathsf{R} = 0 \quad \text{and} \quad \dot{h}^\mathsf{L} < 0 < \ddot{h}^\mathsf{R}. \quad (19)$$

This gives rise to a more dramatic type of bifurcation depicted in figure 5. Again, on one side of the bifurcation a smooth orbit resides in $x > 0$, but on the other side the bifurcating orbit impacts Σ and crosses into $x < 0$. The outward segment of the orbit jumps discontinuously from $x > 0$ to $x < 0$ and the limit cycle is destroyed, therefore this can be termed a *catastrophic sliding bifurcation*.
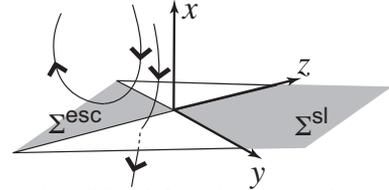
Fig. 5. Catastrophic sliding bifurcation at a visible tangency.

Under variation of a single parameter a grazing limit cycle will not generically intercept the two-fold point $x = y = z = 0$, however, a limit cycle with a sliding orbit may do. The different local sliding topologies are shown in figure 3. From these we can immediately infer a new class of catastrophic sliding bifurcations.

Consider a limit cycle in $x \geq 0$, with a sliding segment that intersects the singularity. The sliding segment begins with an impact point in Σ^{sl}, and ends at the singularity where the dynamics is nonunique: the orbit may be ejected into $x > 0$, or ejected into $x < 0$, or it may follow the sliding vector field (12) into Σ^{esc}. This sliding segment in Σ^{sl} is part of a special sliding orbit: the stable manifold of the saddle-like field for $vw < 1$, and the strong stable or weak unstable directions of the node-like fields for $vw > 1$. This singular orbit constitutes the degenerate point of a bifurcation: as the impact point of a limit cycle passes through the special orbit, the ejection point of the limit cycle moves from S^R to S^L. On one side of the bifurcation the orbit is ejected from Σ into $x > 0$, on the other side it is ejected into $x < 0$ and does not return to $x \geq 0$, thus the limit cycle is destroyed, constituting a catastophic sliding bifurcation.
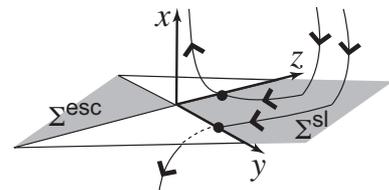
Fig. 6. Catastrophic sliding bifurcation at a visible two-fold.

We have described these scenarios as they occur for a limit cycle that resides in $x \geq 0$ and transect S^R. Due to symmetry in the visible two-fold system these bifurcations occur similarly for limit cycles in $x \leq 0$ that transect S^L.

5. THE VISIBLE-INVISIBLE TWO-FOLD
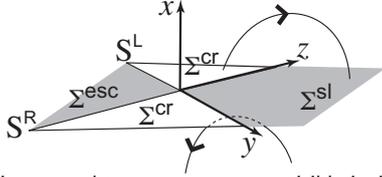
Fig. 7. Coordinates and tangency sets at a visible-invisible two-fold.

A vector field with transverse visible and invisible tangency sets (figure 7) has the local form

$$\begin{pmatrix} \dot{x} \\ \dot{y} \\ \dot{z} \end{pmatrix} = \left\{ \begin{pmatrix} -y \\ 1 \\ v \end{pmatrix} \text{ for } x > 0, \begin{pmatrix} z \\ -w \\ -1 \end{pmatrix} \text{ for } x < 0 \right\} \quad (20)$$

equivalent to the system in section 1 with $\lambda = -\mu = +1$. The sliding vector field quantities (13-15) satisfy

$$\begin{aligned} \Delta &= 1 - wv \\ \mathbf{d}_\pm &= \begin{pmatrix} 1 \\ \delta_\pm + w \end{pmatrix} = \begin{pmatrix} \delta_\pm - v \\ -1 \end{pmatrix} \\ \delta_\pm &= \tfrac{1}{2}\left(v - w \pm \sqrt{(v+w)^2 - 4} \right). \end{aligned} \quad (21)$$

The eigendirections $\mathbf{d}_\pm$ are real for $|v + w| > 2$ and both lie in the same quadrant of Σ: Σ^{sl} or Σ^{esc} for $v + w > 0$, and Σ^{cr} for $v + w < 0$. The cases with $v + w > 0$ are shown in figure 8: the saddle-like case $vw > 1$ in (i), the repulsive node-like case $vw < 1$, $v > w$ in (ii), and the attractive node-like case $vw < 1$, $v < w$ in (iii). For $|v + w| < 2$, in (iv), the eigenvalues are complex and the sliding field is focus-like.

The real eigenvalue cases with $v + w < 0$ have their eigendirections lying in Σ^{cr}, outside of the domain of the sliding vector field. Therefore, as shown by Teixeira (1993), they are topologically equivalent to the focus-like case with no real eigenvalues.
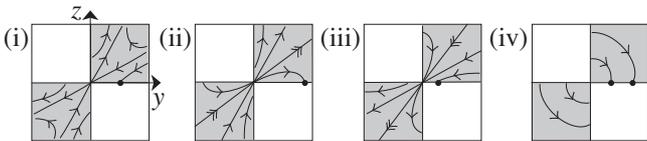
Fig. 8. The sliding vector field near a visible-invisible two-fold, implied by (21). Ejection points are indicated by dots. For $|v + w| > 2$ and $v + w > 0$ we show: (i) the saddle-like case $vw > 1, v + w > 0$; (ii) the repulsive node-like case $vw < 1$, $v > w$; (iii) the attractive node-like case $vw < 1$, $v < w$. For $|v + w| > 4$ we show: (iv) the focus-like case $|v + w| < 2$, topologically equivalent to cases with $|v + w| > 2$ and $v + w < 0$.

As we did in section 4, now consider a limit cycle, at least part of which is a sliding segment, that approaches close to a twofold with the local approximation above. The limit cycle may generically intercept the two-fold point in different ways depending on the sliding vector field (12).

If the sliding vector field is saddle-like (figure 8(i)) there are two ways a limit cycle may contain the two-fold, illustrated in figure 9. In 9(i), the nongeneric case is a smooth

limit cycle, contained in Σ, with a homoclinic connection to the singularity. On one side of the bifurcation is a smooth limit cycle in Σ, on the other side the orbit gains an ejection point on S^L and is ejected into $x < 0$. In 9(ii), the nongeneric case is a limit cycle in $x \leq 0$, with a sliding segment on Σ^{sl} that intercepts the two-fold point. On one side of the bifurcation a limit cycle with a sliding segment and ejection point on S^L resides in $x \leq 0$, on the other side there is no ejection point so the outflowing orbit is confined to Σ^{sl}. In either case the limit cycle is destroyed by what constitutes the same catastrophic sliding bifurcation, unfolding in different directions.
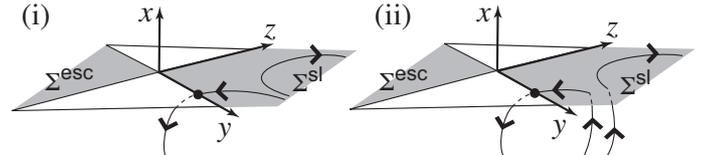
Fig. 9. Catastrophic sliding bifurcation at a visible-invisible two-fold: (i) for a sliding orbit, (ii) for an orbit impacting from $x < 0$.

If the sliding vector field is attractive node-like (figure 8(iii)) then on one side of the bifurcation a limit cycle exists in $x \leq 0$, with a sliding segment that ends in an ejection point on S^L, on the other side the orbit enters the two-fold point. This is illustrated in figure 10. Note the orbit entering the two-fold is stable to perturbation because a set of orbits all flow into the two-fold point around the stable eigendirection. After the impact point crosses the strong eigendirection, the sliding orbit segment always intercepts the singularity in finite time. The forward-time dynamics at the singularity is non-unique according to Filippov's convention, so in this setting the limit cycle is destroyed, and replaced by nondeterministic evolution – the vector field is not uniquely defined at the two-fold point.
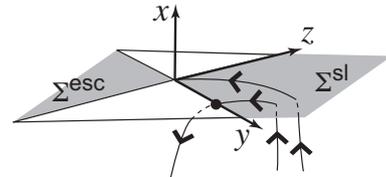
Fig. 10. Nondeterministic sliding bifurcation at a visible-invisible two-fold.

6. THE TEIXEIRA SINGULARITY
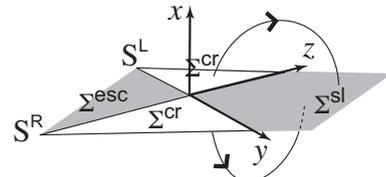
Fig. 11. Coordinates and tangency sets at the Teixeira singularity.

A vector field with transverse invisible tangency sets, the Teixeira singularity (figure 11), has the local form

$$\begin{pmatrix} \dot{x} \\ \dot{y} \\ \dot{z} \end{pmatrix} = \left\{ \begin{pmatrix} -y \\ 1 \\ v \end{pmatrix} \text{ for } x > 0, \begin{pmatrix} z \\ w \\ 1 \end{pmatrix} \text{ for } x < 0 \right\} \quad (22)$$

equivalent to the system in section 1 with $\lambda = \mu = +1$.

The sliding vector field quantities (13-15) become

$$\Delta = vw - 1$$
$$\mathbf{d}_\pm = \begin{pmatrix} 1 \\ \delta_\pm - w \end{pmatrix} = \begin{pmatrix} \delta_\pm - v \\ 1 \end{pmatrix} \qquad (23)$$
$$\delta_\pm = \tfrac{1}{2}\left(v + w \pm \sqrt{(v-w)^2 + 4} \right).$$

The eigendirections are real and lie in different quadrants of Σ, but conversely to the visible two-fold, $\mathbf{d}_+$ lies in Σ^{sl} or Σ^{esc}, and $\mathbf{d}_-$ lies in Σ^{cr}.

Figure 12(i) shows the saddle-like case $vw < 1$, for which $\mathbf{d}_+$ is the repelling eigendirection. There are two node-like cases $vw > 1$: if $v + w > 0$ the origin is a repelling node with $|\delta_+| > |\delta_-|$, figure 12(ii); and if $v + w < 0$ the origin is an attractive node with $|\delta_+| < |\delta_-|$, figure 12(iii).
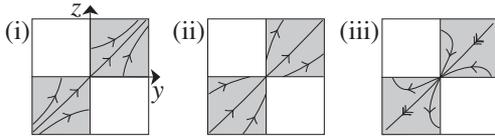
Fig. 12. The sliding vector field near a Teixeira singularity, implied by (23): (i) the saddle-like case $vw < 1$, and the node-like cases $vw > 1$ with (ii) $v, w > 0$, (iii) $v, w < 0$.

The Teixeira singularity exhibits none of the catastrophic sliding bifurcations of sections 4-5, because it lacks any visible tangencies to eject orbits from Σ. However, the dynamics around the Teixeira singularity is interesting for its own reasons. It consists of orbits in $x > 0$ and $x < 0$ that continually map back onto the switching manifold Σ through any number of crossings, resulting in piecewise-smooth orbits that spiral around the singularity.

The following theorem was proven by Jeffrey and Colombo (2009).

THEOREM: *Orbits in the neighborhood of a Teixeira singularity satisfy the following:*

(i) *If $vw > 1$ and $v, w < 0$: any orbit of (22) crosses Σ an infinite number of times. There exist a pair of invariant surfaces that meet at the singularity.*
(ii) *If $vw < 1$ or $v > 0$ or $w > 0$: any orbit of (22) crosses Σ a finite number of times.*

Furthermore, if N is the number of times an orbit may cross Σ:
LEMMA

(i) *if $v > 0$: then $N \leq 1$, crossing is in $y < 0 < z$,*
(ii) *if $w > 0$: then $N \leq 1$, crossing is in $z < 0 < y$,*
(iii) *if $0 < vw < 1$ and $v, w < 0$: then $N \geq 1$.*

Here we review briefly the mapping that provides this result and reveals the rich dynamics of the Teixeira singularity.

To label points on Σ let $m \in \mathbb{Z}$, then let every $\mathbf{x}_{2m}$ be the starting point of an orbit segment in $x > 0$, let every $\mathbf{x}_{2m-1}$ be the starting point of an orbit segment in $x < 0$. The vector field in $x > 0$ reflects points in $\{\Sigma : y < 0\}$ obliquely into $\{\Sigma : y > 0\}$, along the direction $(0, 1, v)$. That is, it affects a map on the Σ plane:

$$\begin{pmatrix} y_{2m+1} \\ z_{2m+1} \end{pmatrix} = \begin{pmatrix} -1 & 0 \\ -2v & 1 \end{pmatrix} \begin{pmatrix} y_{2m} \\ z_{2m} \end{pmatrix}. \qquad (24)$$

Similarly, the vector field in $x < 0$ reflects points in $\{\Sigma : z < 0\}$ obliquely into $\{\Sigma : z > 0\}$, along the direction $(0, w, 1)$, affecting a map on the Σ plane:

$$\begin{pmatrix} y_{2m} \\ z_{2m} \end{pmatrix} = \begin{pmatrix} 1 & -2w \\ 0 & -1 \end{pmatrix} \begin{pmatrix} y_{2m-1} \\ z_{2m-1} \end{pmatrix}. \qquad (25)$$

We can apply these maps in an alternating sequence to points in Σ^{cr}. Points in Σ^{esc} can be considered start points of a sequence beginning with either of the two maps. Similarly points in Σ^{sl} can be considered end points of a sequence ending with either of the two maps. The finite length of iterations makes it difficult to understand the qualitative dynamics of the system directly from (24)-(25), such as asymptotic stability and winding numbers.

However, because the tangency sets are straight lines and the composition of reflections is a rotation, the dynamics is easily understood by studying the problem in polar coordinates. Rather than considering the polar angle of a point in Σ we consider its tangent as measured from the boundary of Σ^{esc}:

$$T_{2m} = \frac{z_{2m}}{y_{2m}} \qquad T_{2m+1} = \frac{y_{2m+1}}{z_{2m+1}}. \qquad (26)$$

T_m is positive for points $\mathbf{x}_m$ in Σ^{sl} and Σ^{esc}, negative in Σ^{cr}, and zero on the boundary of Σ^{esc}. Moreover it is well-defined except on the boundary of Σ^{sl} (where sliding dynamics apply).

The tangents map according to

$$T_{2m+1} = \frac{1}{2v - T_{2m}} \qquad T_{2m} = \frac{1}{2w - T_{2m-1}} \qquad (27)$$

obtained from (24) and (25) respectively. The radial map, $R_m = \sqrt{y_m^2 + z_m^2}$, is easily derived and will not be our main concern, (see Jeffrey and Colombo (2009) for more).

Clearly from (27), a positive v or w implies that points in Σ^{cr} ($T_m < 0$) are mapped into Σ^{sl} ($T_m > 0$) after at most two iterations, or one iteration if both v, w are positive. This provides the Lemma, and part (i) of the Theorem.

Iterates of (27) lie in Σ^{cr} if $2v < T_{2m} < 0$ and $2w < T_{2m-1} < 0$, which limits the angle subtended by T_m to the boundaries of Σ^{esc}. So long as these conditions hold for the mth and $(m+1)^{th}$ iterate, we can compose the maps (24-25) into a second return map with the concise form

$$\tau_{n+2} = \frac{\tau_n - 2}{2vw(\tau_n - 2) + 1}, \qquad (28)$$

for $T_{2m} = v\tau_{2m}$ and $T_{2m-1} = w\tau_{2m-1}$. Thus the maps $T_{2m} \mapsto T_{2m+2}$ and $T_{2m-1} \mapsto T_{2m+1}$ respectively have stable equilibria T_S^{R} and T_S^{L}, given by

$$\frac{T_S^{\mathsf{R}}}{v} = \frac{T_S^{\mathsf{L}}}{w} = 1 - \sqrt{1 - \frac{1}{vw}} \qquad (29)$$

and unstable equilibria T_U^{R} and T_U^{L} given by

$$\frac{T_U^{\mathsf{R}}}{v} = \frac{T_U^{\mathsf{L}}}{w} = 1 + \sqrt{1 - \frac{1}{vw}}. \qquad (30)$$

These are invariant manifolds of the maps (24-25), and exist only in $T_{U,S}^{\mathsf{R,L}} < 0$, which means in Σ^{cr}, for $v, w < 0$. The stable manifolds $T_S^{\mathsf{R,L}}$ enclose Σ^{esc}, while the unstable manifolds $T_U^{\mathsf{R,L}}$ enclose Σ^{sl}, and each of the pairs $\{T_S^{\mathsf{R}}, T_U^{\mathsf{L}}\}$ and $\{T_U^{\mathsf{R}}, T_S^{\mathsf{L}}\}$ forms a straight line through the origin since

$T_S^R T_U^L = T_U^R T_S^L = 1$. These invariant manifolds imply part (ii) of the Theorem.

The radial map satisfies $R_{m+2} > R_m$ on the stable manifolds and $R_{m+2} < R_m$ on the unstable manifolds. Therefore points in T_U move toward the singularity, while points in T_S move away from it, as illustrated in figure 13.
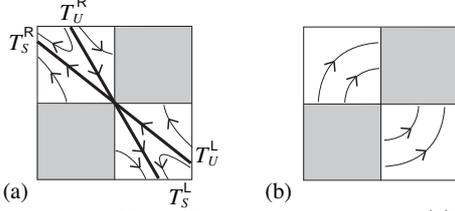
Fig. 13. Invariant manifolds of the second return map: (a) when $vw > 1$, $v, w < 0$ the directions $T_{U,S}^{R,L}$ form two stable and two unstable manifolds in the crossing regions, which are respectively repelling and attracting with respect to the central Teixeira singularity. (b) when $vw < 1$ or $v > 0$ or $w > 0$ all points map from the escaping region to the sliding region in finite time.

As a consequence of the construction in section 2, functions

$$x(y,z) = \frac{vy^2 + wz^2 - 2vwyz}{2\gamma(1 - vw)} \qquad (31)$$

prescribe invariant surfaces around the singularity, with $\gamma = \{v \text{ for } x > 0, -w \text{ for } x < 0\}$. The invariant manifolds $T_{S,U}^{R,L}$ extend into two continuous invariant surfaces U and S described by (31). These are a pair of cones which are smooth except at their intersections $T_{U,S}^{R,L}$ with Σ – a 'nonsmooth diabolo' (figure 14), comprised of an attractive cone S that encloses Σ^{esc} within a basin of repulsion from the singularity, and a repelling cone U that encloses Σ^{sl} within a basin of attraction towards the singularity. Both cones have their apex at the origin.
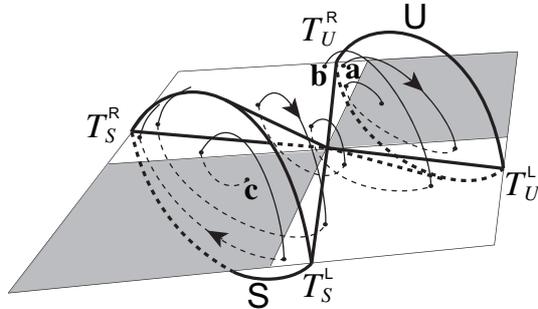
Fig. 14. The nonsmooth diabolo: invariant manifolds (31) near a two-fold singularity. The three qualitatively different types of orbit are shown. a: in the region of attraction bounded by unstable cone U, b: between the invariant cones, c: in the region of repulsion bounded by stable cone S.

Finally, note that a single parameter vw determines both: the existence of invariant manifolds crossing the switching manifold, and whether the sliding vector field is saddle-like or node-like. The existence of the invariant manifolds $T_{U,S}^{R,L}$ coincides with node-like sliding, and the absence of invariant manifolds coincides with saddle-like sliding.

7. CONCLUDING REMARKS

The two-fold singularity introduces a new class of global bifurcations with striking effects on switching dynamics and clear ramifications for control. Why, then, have two-folds not been reported in control systems to date? It is possible either that their dynamics is so benign as to go undetected. This is possible for the Teixeira-singularity where the dynamics changes smoothly under parameter variation, but it is unlikely for folds with visible grazing, because catastrophic bifurcations of orbits can then occur. A second possibility is that the two-folds have been seen, but not recognized, because their dynamics was not understood. We hope to address that with the present work. Furthermore, the two-folds can themselves be used as a design tool. For example, the bifurcation of invariant manifolds near the Teixeira-singularity at $vw = 1$ implies the birth of a limit cycle, residing near the invariant manifolds and with a size controlled by vw.

This paper attempts to stimulate further study of grazing singularities in piecewise-smooth dynamical systems, by exhibiting the behaviour by which the singularities can be recognised in real systems. The growing theory of nonsmooth bifurcations, and the study of real nonsmooth models, would both greatly benefit from further study into how these singularities appear in, and affect, the stability of real world mechanical, biological, and electrical systems.

REFERENCES

di Bernardo, M., Budd, C.J., Champneys, A.R., and Kowalczyk, P. (2008). *Piecewise-Smooth Dynamical Systems: Theory and Applications*. Springer.

di Bernardo, M., Garofalo, F., Glielmo, L., and Vasca, F. (1998). Switchings, bifurcations, and chaos in dc/dc converters. *IEEE Trans. Circuits Syst. I*, 45, 133–141.

Filippov (1988). *Differential Equations with Discontinuous Righthand Sides*. Kluwer Academic Pulbishers.

Galvanetto, U. (1997). Bifurcations and chaos in a four-dimensional mechanical system with dry friction. *Journal of Sound and Vibration*, 204, 690–695(6).

Jeffrey, M.R. and Colombo, A. (2009). The two-fold singularity of discontinuous vector fields. *SIADS*, in press.

Kowalczyk, P. and di Bernardo, M. (2005). Two parameter degenerate sliding bifurcations in filippov systems. *Physica D*, 204, 204–229.

Kunze, M. (2000). *Non-Smooth Dynamical Systems*. Springer.

Leine, R.I. and Nijmeijer, H. (2004). *Dynamics and Bifurcations of Non-Smooth Mechanical Systems*. Springer-Verlag.

Lur'e, A.I. and Postnikov, V.N. (1944). On the theory of stability of control systems. *Appl. Math. Mech.*, 8.

Teixeira, M.A. (1990). Stability conditions for discontinuous vector fields. *J. Diff. Eq.*, 88, 15–29.

Teixeira, M.A. (1993). Generic biurcation of sliding vector fields. *J. Math. Anal. Appl.*, 176, 436–457.

Zhusubalyev, Z.T. and Mosekilde, E. (2003). *Bifurcations and Chaos in Piecewise-Smooth Dynamical Systems*. Mainland Press.